

HiSST: 4th International Conference on High-Speed Vehicle Science Technology 22 -26 September 2025, Tours, France



Numerical and Experimental Studies on Rotating Detonation Engines in ONERA-Pprime Collaboration

Dmitry Davidenko¹, Thomas Gaillard¹, Pierre Hellard^{1,2}, Pierre Vidal², Ratiba Zitoun², Patrick Berterretche²

Abstract

This study addresses the problematics of improving operating characteristics of a rotating detonation combustor (RDC) by means of injector optimisation. An injector concept with partial premixing of propellants in a small prechamber was developed and optimised at ONERA using numerical simulations. It was realised as the ITEM injector for a laboratory-scale RDC tested at the GAP facility of Pprime Institute, together with a commonly used injector design. The obtained results show superior detonation characteristics with the partially-premixed injection. The annular gap width is another important factor for detonation wave stability. Numerical simulations with the CEDRE code of ONERA demonstrate a fairly good agreement with the experimental results regarding detonation propagation characteristics and the visualised wave structure. The simulation results confirm good mixing ahead of the detonation front and low deflagration losses.

Keywords: rotating detonation chamber, methane-oxygen injection, partially-premixed injection

Nomenclature

D – detonation wave velocity ER – equivalence ratio e – annular gap width *T* – temperature *t* – time

Y – mass fraction

y – distance from the injection plane

Greek

 η_{mix} – mixing efficiency θ – azimuthal angle

Subscripts

CJ – Chapman-Jouquet conditions

1. Introduction

Over the past decades, Rotating Detonation Engines (RDEs) have garnered renewed interest due to their potential for enhanced thermodynamic efficiency and reduced component size compared to conventional chemical propulsion systems [1]. The RDE operating principle consists in the continuous propagation of detonation waves in an annular combustion chamber. The detonation waves consume a layer of fresh propellant mixture formed near the injector wall. Fresh mixture compression by the shock front of a detonation wave creates conditions for thermodynamically more efficient combustion with respect to a constant-pressure combustor. The potential efficiency gain in the rocket mode depends on the equivalence ratio, chamber pressure, and ambient pressure [2].

In France, active studies on RDE were started at Pprime Institute and MBDA France in 2000s, and at ONERA in 2013. The GAP facility, unique in France, was created at Pprime specifically for testing subscale rotating detonation combustors (RDC). Research activities at ONERA were focused on numerical investigations of the injection and mixing processes as well as on modelling and numerical analysis of RDC operation. Since 2021, ONERA and Pprime are collaborating to carry out numerical and experimental studies of a laboratory-scale RDC. A commonly supervised PhD study [3] allowed

HiSST-2025-255 Numerical and Experimental Studies on RDE in ONERA-Pprime Collaboration Copyright © 2025 by author(s)

¹ DMPE, ONERA, Université Paris Saclay, Palaiseau, F-91123, France, dmitry.davidenko@onera.fr

² Institut Pprime (UPR 3346 CNRS), Futuroscope-Chasseneuil, F-86960, France, pierre vidal@ensma.fr

designing and testing an optimized injector with partial premixing of gaseous methane and oxygen. The obtained results show superior detonation characteristics in terms of propagation velocity and stability with this injector as compared to another design for separate propellant injection. The main results of this PhD study are presented below.

ONERA is also collaborating with the Institute of Space Propulsion of DLR in the scope a common PhD thesis to study operation of a laboratory-scale RDC fed with gaseous hydrogen and oxygen. A specific paper on this study is presented to HiSST 2025.

Numerous experimental studies have been realised worldwide with different RDC configurations, including the injection principle and the combustor duct profile, as well as with various injection conditions. Most of the known studies report an important deficit of the detonation propagation velocity with respect to the theoretical value. This deficit can be due to several loss factors including excessive confinement, wall viscous interactions, and parasitic deflagration. Nevertheless, the refill and mixing processes are always critical factors defining the fresh mixture quality because their duration is strictly limited by the period between consecutive detonations. Trying to improve detonation propagation characteristics, different injector designs have been tested. Some of them are based on fully separate injection of fuel and oxidizer and represent different combinations of orifices and slots [4-8]. Another group uses premixed injection trying to avoid the flashback [9,10]. Finally, different types of partially premixed injection were proposed as a trade-off between the safety of the separate injection and the mixture quality of the premixed injection [11-13]. This paper presents results of numerical and experimental studies with separate and partially premixed injection demonstrating advantages of the latter principle.

2. Development of an optimised design for the RDC injector

Injector is a key element of an RDC because the fresh mixture quality it produces has a direct effect on detonation propagation characteristics and hence on the overall RDC performance. Another important criterion is the loss of the injection total pressure due to the internal loss factors and the interactions between the propellant jets and during their expansion in the RDC duct. These factors have been studied at ONERA since 2013 by modelling and numerical simulations, trying to find an optimum injector design for a rocket-type RDC [14].

To simplify the problem, the injector is considered as an ensemble of regularly arranged elements of identical shape, which can be repeated along the azimuthal and radial directions on the injector face. A first design of semi-impinging type was optimised to obtain good mixing and acceptable total pressure loss by simulating a cold flow of gaseous H₂ and O₂ [15]. However, by simulating a rotating detonation with this semi-impinging injector, some important drawbacks are identified [16]. First, the mixing process is not sufficiently fast during a short period between consecutive detonation waves. Second, the injector response to the sharp pressure perturbations, caused by passing detonation waves, is not the same for both propellants, so there exists an important disbalance of their flow rates during the injection process, which finally leads to a stratified propellant distribution in the fresh mixture layer.

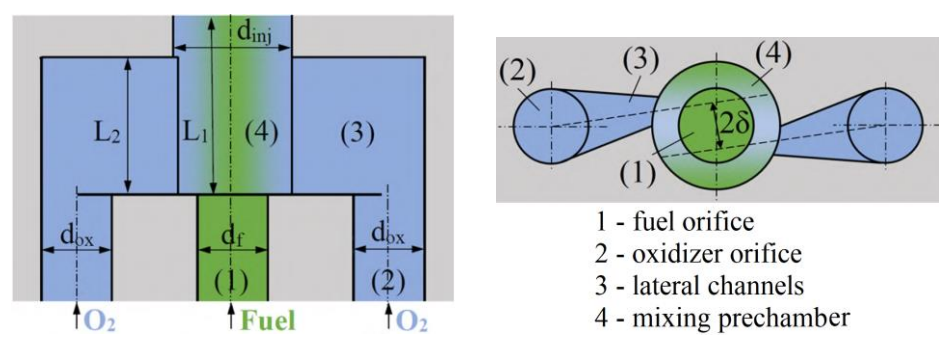


Fig 1. Injector element design with partial premixing of injected propellants

Injector operation can be improved by putting into contact the injected propellants in a confined volume so that their contact surface become developed before they enter the combustion chamber. For this purpose, the following design has a prechamber as shown in Fig. 1. A central orifice (1) and two lateral orifices (2) are respectively used for fuel and oxidizer feeding. The side orifices are connected to the prechamber (4) by lateral channels (3). These channels have narrow openings to the prechamber,

which are shifted from each other by 2δ . This shift is specifically chosen to obtain the most favourable conditions for mixing, once the propellants leave the injector. The entire design is compact and allows placing injection elements close to each other. The oxidizer orifices may be connected up to four neighbouring elements by lateral channels to form a dense arrangement and to simplify oxidizer distribution. This design is patented by ONERA [17].

Operation of the injectors of both types was simulated in a simple linear configuration. Twenty-one injection elements are aligned in a 51.5 mm long and 2.4 mm wide computational domain. Gaseous H₂ and O₂ are injected at 300 K and in stoichiometric proportions. The average mass flux through the chamber cross section is of 100 kg/s/m². Simulated flowfields are shown in Fig. 2. Propellants are injected from the bottom. Injection is fully separate with semi-impinging elements (Fig. 2a) because the propellants start mixing in the chamber. The propellant jets, shown in blue, form a fresh mixture layer in a zone near the injector plane where a detonation wave propagates from left to right. The flowfield is periodic in the horizontal direction so the detonation propagation cycles are repeated every 20 µs. The upper boundary is open so the combustion products can freely leave the chamber.

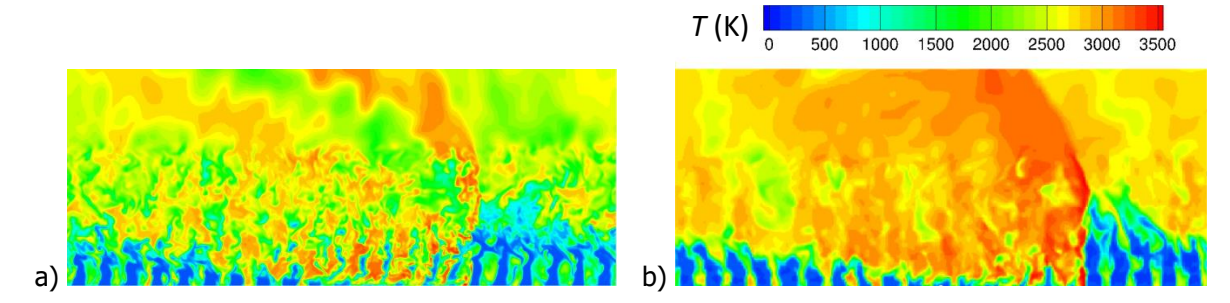


Fig 2. Instantaneous temperature fields in the mid-plane of the computational domain with separate injection (a) and partially-premixed injection (b)

In both flowfields, the detonation wave is situated in the right-hand portion. Its location is marked by consumption of the fresh mixture and appearance of hot combustion products. This effect is more pronounced with the partially-premixed injection (Fig. 2b), indicating a stronger wave with more intense combustion. Indeed, the detonation propagation velocity is about 2170 m/s with the separate injection, against 2600 m/s with the partially-premixed injection.

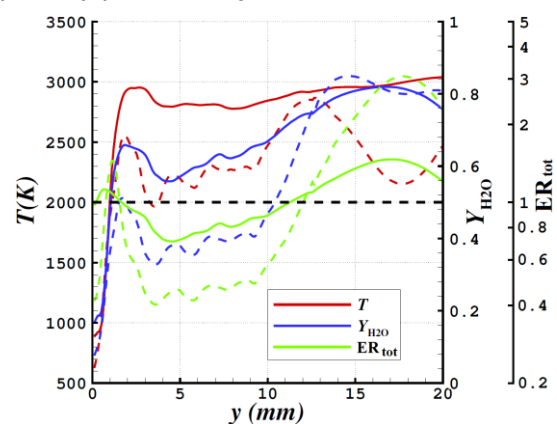


Fig 3. Profiles of phase-averaged flow properties versus distance from the injection plane 16 mm past the detonation wave. Dashed lines correspond to the separate injection and solid lines to the partially-premixed injection

Another evidence of the advantage of the partially-premixed injection is presented by the profiles in Fig. 3. They are extracted from phase-averaged flowfields where the detonation front is kept at a fixed position. These profiles correspond to the combustion products 16 mm past the detonation wave. The temperature profiles show a 700 K reduction within the upper and lower parts for the separate injection, whereas the other case gives an almost constant level. The profile of H₂O mass fraction (Y_{H2O}) also shows a significant reduction in the lower part for the separate injection. Both these negative effects can be caused by a less effective propellant mixing within the fresh mixture layer. However, the profiles of total equivalence ratio (ERtot, defined from the balance of H and O atoms of all mixture components),

indicate an important stratification of propellant masses with the separate injection: the mixture is lean (ER_{tot} \approx 0.4) in the lower part and rich (ER_{tot} \leq 3) in the upper part. With the partially-premixed injection, ERtot varies between 0.7 and 1.5.

The concept of partially-premixed injection was later realised in a different form, more convenient for classical manufacturing technology, and experimentally tested at Pprime. This corresponds to the ITEM injector described in the next section.

3. Experimental tests of a methane-oxygen RDC

3.1. Experimental setup

Experimental studies of a methane-oxygen RDC were conducted on the GAP facility of the Pprime Institute. A photo of the experimental RDC on the test bench is shown in Fig. 4. This RDC has a straight annular duct with the following dimensions: a length of 110 mm and an outer diameter of 80 mm. The radial gap of the annulus can be set to 5 or 10 mm by changing the centre body. The chamber structure is made of stainless steel and there is an optional outer wall of quartz for optical access.



Fig 4. Experimental RDC with a transparent wall on the GAP test bench

The RDC can be equipped with two different injectors, whose elements are shown in Fig. 5. The first configuration, referred to as ITEM (Injector To Enhance Mixing), is a O2-CH4-O2 triplet with a prechamber to partially mix the propellants before injection into the RDC. The second one, referred to as TRIPLET, is a CH₄-O₂-CH₄ triplet for separate injection, so the jets impinge onto each other inside the RDC. This latter configuration is representative of several published examples [7,8]. Each injector consists of 72 elements with a total injection area of 226 mm² for ITEM and 202 mm² for TRIPLET.

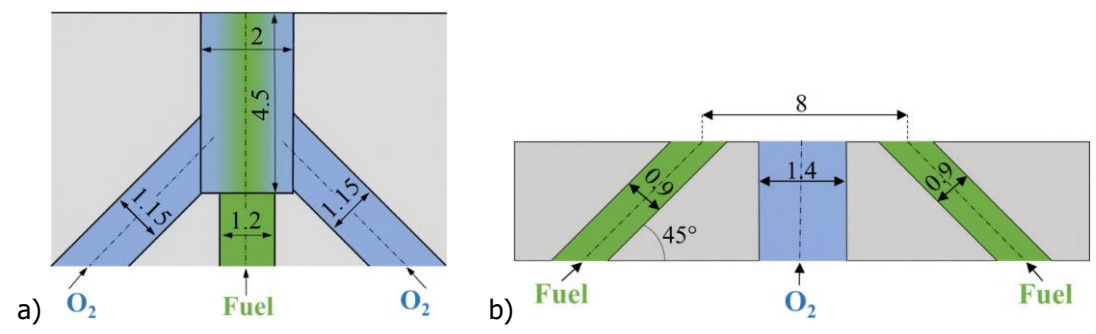


Fig 5. Injector element configurations with dimensions in mm: a) ITEM, b) TRIPLET

The fuel and oxidizer are fed into plenums to distribute their flow among the injector elements. The propellant flow rates are measured in the feed lines using choked throats with an uncertainty of 1.3%, which is verified in cold-flow tests using Coriolis flow meters. Stable flow rates can be ensured during at least 300 ms based on stable pressure in the fuel and oxidizer plenums.

Kistler 603B high-frequency pressure sensors are used for dynamic pressure measurement at different locations on the outer wall. Backend chemiluminescence imaging is performed with a Phantom TMX UV camera. The camera recording frequency is 230 kHz, and the spatial resolution is 0.3 mm/px. The exposure time is set to 100 ns to limit the blurring effect (less than 1 pixel). A 300-500 nm filter is installed on the camera to cover the spectral range of OH* and CH* chemiluminescence.

HiSST-2025-255 Page | 4 D. Davidenko, T. Gaillard, P. Hellard, P. Vidal, R. Zitoun, P. Berterretche Copyright © 2025 by author(s)

Both of these techniques provide data for detonation propagation characterisation. Standard Fourier transform helps to build spectrograms of pressure sensor signals. Phase difference between the signals is used to detect the number of detonation fronts and the propagation direction. The signal shape is also used for comparison with simulation results.

Fast camera recordings of the backend view are postprocessed to track propagating fronts. An automatic algorithm [18] is used to generate an angular position versus time diagram that reveals the front dynamics and possible transitions between different propagation regimes. A 2D Fourier transform applied to such a diagram provides data on the number of fronts and their rotation frequency.

With a transparent wall, camera recording of the side view gives important information about the wave structure and the detonation front height. Instantaneous and phase-averaged images can be compared with simulated flowfields for a conjugate analysis.

3.2. Operation regimes and detonation velocity

Operation regimes are determined for the experimental RDC with the ITEM injector and two annular gaps, e = 5 and 10 mm, as well as with the TRIPLET injector and e = 10 mm (no stable detonation propagation was obtained with e = 5 mm). Figure 6 shows operation maps for the three tested configurations depending on the total mass flow rate of injected propellants and the global equivalence ratio (ER). Stable detonation modes (colour symbols) correspond to 1, 2 or 3 co-rotating fronts. The deflagration mode (black cross) does not produce detectable pressure peaks. The unstable modes (black diamonds) correspond to counter-rotating fronts or chaotic pressure fluctuations.

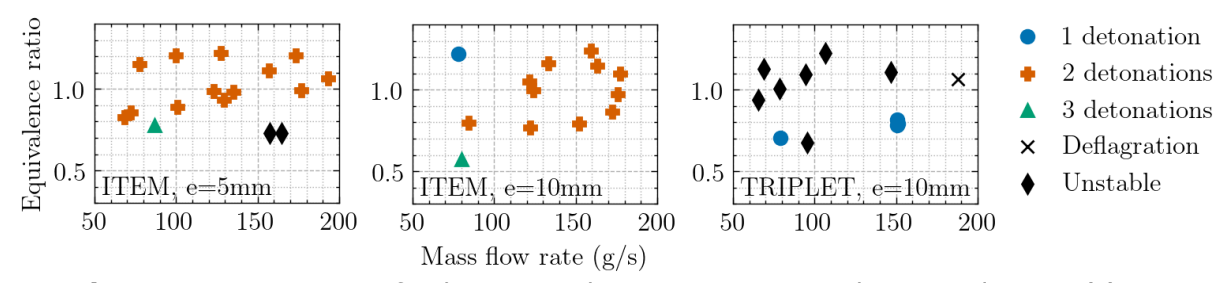


Fig 6. Operation regimes for the ITEM and TRIPLET injectors and two annular gaps (e)

For the ITEM injector and 5 mm annular gap, 2 co-rotating waves are mostly observed, except for the leanest condition ER = 0.75 and a mass flow rate of 85 g/s. The main regime remains after changing the annular gap to 10 mm, however 1 or 3 waves are also obtained at flow rates lower than 100 g/s for higher and lower ER. Bigler et al. [19] also report that the number of detonation waves depends on ER. In general, the relationship between ER and the wave number is not well identified. In our study, most of the regimes with the TRIPLET injector are unstable, with only two conditions resulting in 1 stable detonation: a flow rate of 80 g/s with ER = 0.7 and a flow rate of 150 g/s with ER = 0.8.

The apparent detonation velocity was calculated as $D = 2\pi R_j f_D / N_{w_l}$ where f_D is the frequency of detonation wave passages at a pressure sensor, N_w is the number of rotating waves, and R_i is the injector mid radius. The fresh mixture layer is formed near the injector ring regardless of the annular gap. Therefore, D was calculated at $R_i = 37.5$ mm for ITEM and 35 mm for TRIPLET, instead of the mid radius of the chamber annulus.

The ratio of the measured velocity D to the theoretical Chapman-Jouquet speed D_{\square} is linked to the fresh mixture quality in front of the wave. In Fig. 7, the ratio D/D_{CI} obtained in our study is compared with experimental data from the literature for annular RDCs fed with CH₄ and O₂ [5,8,11,19-25]. For consistency, all the data are converted to the same representation, using the mid radius of axial injectors or the chamber mid radius for the radial injections. The D_{\square} speed was computed for the global equivalence ratio of each experiment, assuming a homogeneous CH₄/O₂ mixture at 1 bar and 293 K and equilibrium combustion products composed of chemical species with standard thermodynamic properties.

There is no evident trend of the D/D_{\square} ratio versus the mass flux corresponding to the chamber cross section. With the ITEM injector and 5 mm annular gap, D/D_{CJ} is at the same level as most of the literature data, i.e. about 65% to 70%. However, with the 10 mm gap, D/D_{\Box} reaches 85% to 90% for a wide range of ER. In contrast, with the TRIPLET injector, D/D_{CI} is 52% to 65%. At least a 10% increase in D/D_{\Box} can be achieved with the ITEM injector, compared to published results with other

injector configurations. This improvement could de attributed to the higher mixture quality provided by the optimized ITEM injector.

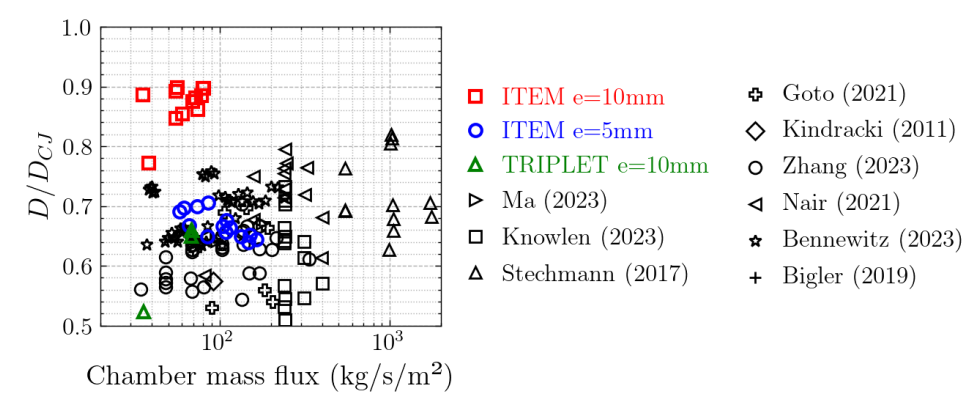


Fig 7. Detonation velocity ratio from experiments with annular RDCs fed with CH₄/O₂

3.3. Detonation front visualisation with the ITEM injector

Direct chemiluminescence imaging was performed with the ITEM injector and two annular gaps (e = 5 and 10 mm). The injection conditions in both cases are: a mass flow rate was of 160 g/s and a global equivalence ratio ER = 1.2. Two co-rotating detonation waves are observed with different velocities: 1600 m/s for e = 5 mm and 2150 m/s for e = 10 mm.

Figure 8 shows phase-averaged images from side-view video recordings though a transparent wall. The luminosity is normalised, so it is not an absolute indicator. Several distinct features can be noted from these images. The highest luminosity is observed near the injector wall for the smaller gap, whereas it is within the upper part of the detonation front for the larger gap. In the first case, the wave is less intense thus the major light emission can originate from the recirculation zone around the propellant jets, as well as from the erosion of a graphite gasket between the injector and the transparent wall. In the second case, the detonation front is the main light source and its intensity correlates well with better propellant mixing in the upper part of the fresh mixture layer; the front is inclined slightly forwards. An oblique shock attached to the detonation front is visible in both cases, and its inclination correlates with the detonation propagation velocity. A slip line between the expanding gases behind the detonation and the shocked gases can also be distinguished. The three waves form a classical configuration. No visible emission is observed within the fresh mixture layer in front of the detonation, meaning that the deflagration is not intense.

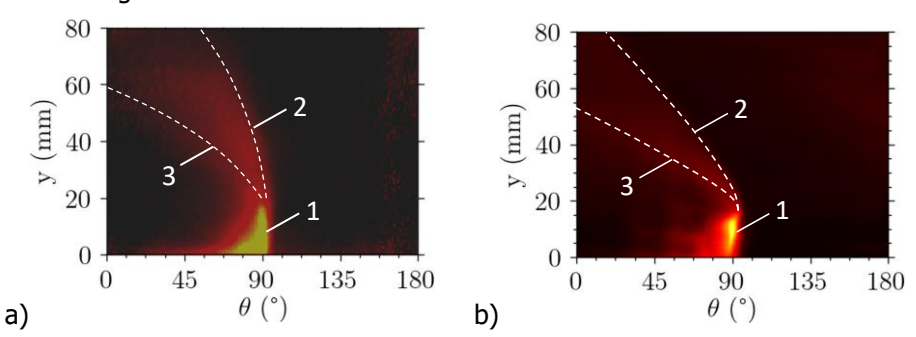


Fig 8. Phase-averaged images from the side-view video recordings for two annular gaps: a) e = 5 mm, b) e = 10 mm. 1 – detonation front, 2 – attached shock, 3 – slip line

Instantaneous images from backend video recordings are shown in Fig. 9 with chamber annulus contours for both cases. The chemiluminescence zone have notable differences. It is more diffused and wider distributed for the smaller gap. This could be due to incomplete burning of the fresh mixture by the weaker detonation, resulting in distributed combustion behind it. On can also see a secondary luminescence zone, which periodically appears after the main one. This can be produced by combustion of residual fresh mixture of a premature ignition of newly injected propellants. With the larger gap, the light emission is more intense and concentrated. The denotation front is localised within the outer part of the cross section, next to the injector ring.

Fig 9. Instantaneous chemiluminescence images of a detonation wave from backend video recordings for two annular gaps: a) e = 5 mm, b) e = 10 mm

Detonation front tracks are visualised by the θ -t diagrams in Fig. 10. For the smaller gap, the two detonation fronts have variable intensity indicated by changing luminosity and inclination of the front tracks; weaker counter-rotating waves are also observed. A 2D Fourier transform of the θ -t diagram in Fig. 10a reveals that the velocity of the counter-rotating waves is about 1000 m/s, which corresponds to acoustic perturbations. These counter-rotating waves are produced by periodic ignitions past the main front, as the one shown in Fig. 9a, as well as by periodic intensifications of the detonation front. With the larger annular gap, the detonation fronts appear very stable without counter-rotating waves (Fig. 10b).

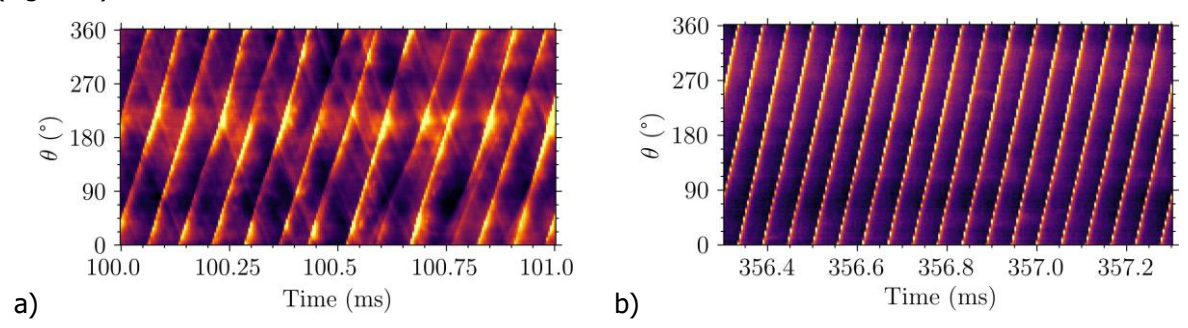


Fig 10. Angular position of the detonation fronts versus time for two annular gaps: a) e = 5 mm, b) e = 10 mm

4. CFD study of the methane-oxygen RDC

A CFD study of the RDC with the ITEM injector and 10 mm annular gap has been carried out in order to obtain a detailed characterisation of the RDC operation under the test conditions described above.

4.1. Computational setup

The CEDRE code of ONERA [26] is used to perform a Large-Eddy Simulation of the reactive flow in an RDC, whose internal geometry corresponds to the experimentally tested model. The computational domain includes three main parts: the injector with the propellant plenums, the chamber duct, and the dump volume for the exhaust flow. The domain covers a half of the RDC within a 180° sector, which is sufficient for the operating regime with 2 stable co-rotating detonation waves. The computational mesh is composed of 26 million tetrahedrons of variable size: 40 µm in the injector, 100 µm in the detonation propagation zone (within a 20 mm distance from the injector plane), and progressively increasing to 800 µm towards the chamber exit. A coarser mesh with 11 million tetrahedrons was also used to verify grid-independence of the numerical solution.

The Navier-Stokes (NS) equations for compressible reactive gas are discretised according to the finite volume method and with second-order accurate spatial schemes. A MUSCL method with the Van Leer slope limiter and the HLLC Riemann solver are applied to evaluate the convective fluxes, whereas a central-differencing scheme is used for the viscous fluxes. The time integration is performed with the Euler implicit scheme and a time step of 2 ns.

The standard Smagorinsky subgrid model is used to treat unresolved turbulent structures. The chemical kinetics of the reacting CH₄/O₂ mixture is modelled with the reduced mechanism by Laurent [27] composed of 62 reactions between 16 chemical species. This mechanism was preliminarily tested by modelling selfignition under the detonation-specific conditions and premixed laminar flame propagation. Temperature-dependent thermodynamic properties of the chemical species are determined using NASA polynomials with standard coefficients. The dynamic viscosity of the chemical species and their mixture are respectively calculated according to the Sutherland law and the Wilke formula. Constant Prandtl and Schmidt numbers are used to evaluate the thermal conductivity and diffusion coefficients for the species, together with mixing laws for the corresponding mixture properties.

The boundary conditions are defined as follows. A total temperature of 293 K and a constant mass flux are specified at the inlet boundaries of the propellant plenums in order to obtain the total mass flow rate of 160 g/s and the global equivalence ratio ER = 1.2. All the walls are considered as adiabatic with slip condition for the velocity. In our previous study [28], it was found that the skin friction and heat exchange on the chamber walls resulted in a small change in the detonation propagation velocity. On the other hand, proper resolution of the boundary layers requires a much finer mesh and consequently an unreasonably high computational cost. Periodicity conditions are set at the radial planes cutting the chamber. Finally, the atmospheric pressure and non-reflecting conditions are imposed over the outflow boundary of the dump volume to evacuate the exhaust gases and shock waves from the chamber.

The initial condition is specifically tailored for faster stabilisation of the detonation propagation. The injector flowfield is taken from a separate cold-flow simulation. The chamber flow is initialised by mapping the flowfield from a 2D simplified configuration.

4.2. Simulation results

The detonation propagation velocity is determined from the simulation results by analysing pressure signals recorded by numerical sensors. The obtained value of 2190 m/s is slightly lower than the experimental velocity of 2205 m/s. Figure 11 shows pressure histories measured at the outer wall of the RDC duct and at 8 mm from the injection plane in comparison with the numerical results. The numerical signal is processed to account for the pressure averaging over the surface of the experimental sensor. It is in good agreement with the experimental signal in terms of frequency and amplitude of the main peaks. Both signals show a secondary peak approximately 15 μ s after the main one, which is caused by a shock train behind the detonation wave.

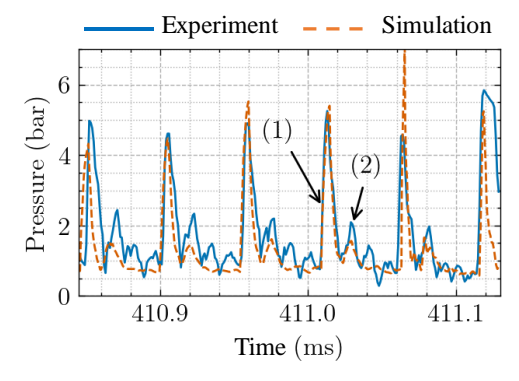


Fig 11. Experimental and numerical pressure histories at the outer wall

An instantaneous temperature field at the injector mid radius, produced by the simulation, is shown in Fig. 12. By comparing it with the experimental image from Fig. 8b, one can note a good resemblance of the wave structures. In particular, the detonation front height and the slopes of the attached shock and slip line. The simulated field shows some other important features. The fresh mixture layer, identified by the low-temperature zone (blue colours), is formed by a series of propellant jets. Some deflagration can be noted along the upper boundary (green colours) due to the contact with burnt gases. Turbulent motions enhance the deflagration by increasing the contact surface. The detonation front is not clearly visible but its localisation can be identified by the fresh mixture consumption. Behind this front, only small pockets of unburnt mixture remain. The injection is recovered at some distance from the front.

The simulation permits to obtain important characteristics of the injection and mixing processes. The ITEM injector is designed to obtain partial propellant premixing at its exit. By time-averaging of the injected composition during several detonation propagation periods, it is found that only about 15% of the mixture mass is near stoichiometry (0.6 < ER < 1.4), whereas 33% is very lean (ER < 0.1), and 21% is rich (ER > 2.8). This low mixing level prevents the detonation from propagating into the injector.

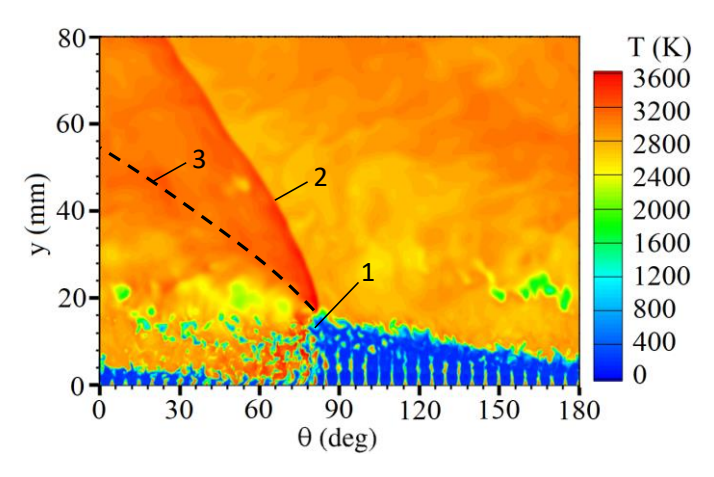


Fig 12. Instantaneous temperature field at the injector mid radius. 1 - detonation front, 2 - attached shock, 3 - slip line

The injection dynamics over a detonation propagation period between two consecutive waves is illustrated in Fig. 13. Each curve corresponds to the injected mass flow rate of one propellant, normalized by the mean flow rate, and represents a phase-average of time histories over 5 propagation periods for 4 evenly distributed injection elements, resulting in 20 injection cycles. The 0 abscissa corresponds to the detonation arrival at the injection hole, so the following pressure jump reduces the mass flow rates during 15% of the period. The injection is restored at about 25% of the period. The O_2 flow rate varies between 100% and 110% of its mean value, whereas the CH₄ flow rate gradually increases from 95% to 115%. During the last 15% of the period, both flow rates change suddenly, resulting in a significant excess of CH₄. Excepting this short disbalance, the injected mass flow rates remain close to the right proportion and would not cause propellant stratification in the fresh mixture layer.

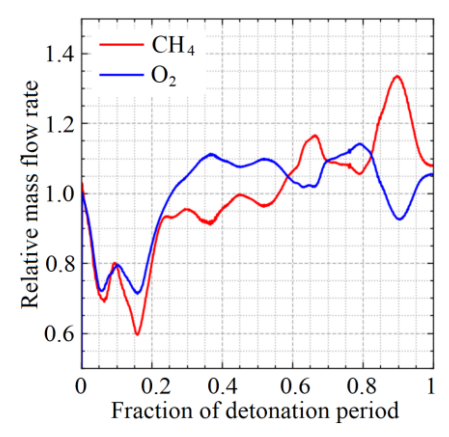


Fig 13. Evolution of the injected mass flow rates related to their mean value over a detonation propagation period

Fresh mixture quality in front of a detonation wave needs to be characterised to complete the analysis. The method applied is known as Phase-Locked Ensemble Average [29] and consists in shifting the saved flowfields in order to match the injection element at which the detonation front is located. The averaged field within a volume surrounding the injection element in front of the detonation wave is used for processing. Taking as an illustration the flowfield in Fig. 12, where the detonation wave is located close to $\theta = 90^{\circ}$, the sector 90° to 95° covering the next injection element corresponds to such a control volume. Mixture quality is evaluated in a control volume cross section at a given distance y from the injection plain. The mixing efficiency is determined by the following formula:

$$\eta_{mix}(y) = \frac{\iint_{S_y} \rho \min(Y_{\text{CH}_4}(1+MR), Y_{\text{O}_2}(1+MR^{-1})) dS_y}{\iint_{S_y} \rho dS_y}$$
 (1)

where ρ is the bulk density, Y_{CH4} and Y_{O2} are the propellant mass fractions, MR is the mixture ratio corresponding to the global ER = 1.2, S_V is the cross-section surface. By this definition, the mixing

HiSST-2025-255 Page | 9
Numerical and Experimental Studies on RDE in ONERA-Pprime Collaboration Copyright © 2025 by author(s)

efficiency is reduced in presence of burnt gases because the denominator represents the entire mass in a cross section.

The profiles of the mixing efficiency and the average ER versus y are traced in Fig. 14a. The mixing efficiency is of 28% at y=0 due to partial premixing in the injector, then gradually increases to 62% at y=12 mm. The following drop is because of increasing fraction of burnt gases at the edge of the fresh mixture layer (y=15 mm). The average ER varies around the nominal level within the fresh mixture layer. A local peak at y=5 mm is due to the previously discussed sudden change in the propellant flow rates at the end of the injection cycle (see Fig. 13).

Considering the whole control volume, the ER distribution by mass is shown in Fig. 14b. Almost 50% of propellants are mixed near stoichiometry (0.6 < ER < 1.4). The overall repartition of the injected propellant masses before their consumption by a detonation is the following: 60% is perfectly mixed, 25% is unmixed, 15% is burnt by deflagration. The remaining unmixed propellants are burnt in an expanding flow of combustion products. Only 0.03% of CH_4 remains unburnt at a distance of 30 mm from the injector. The average total temperature of combustion products is of 98% of its adiabatic value in a homogeneous mixture.

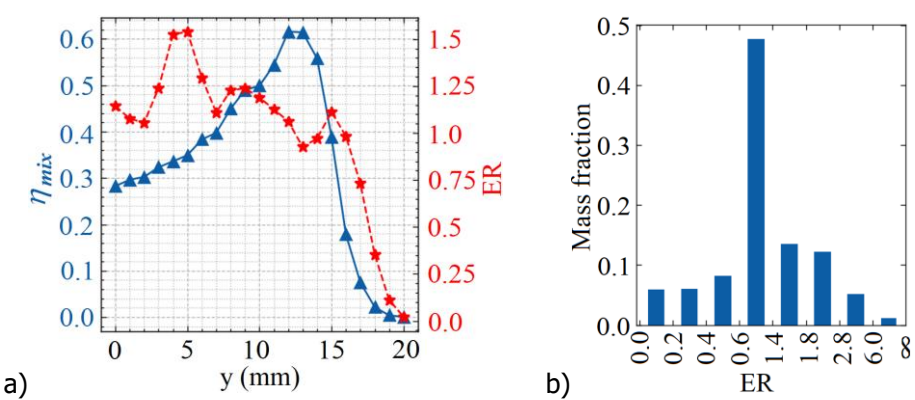


Fig 14. Characteristics of the fresh mixture layer in front of the detonation wave:

a) mixing efficiency and average equivalence ratio versus distance from the injection plane;

b) equivalence ratio distribution by mass

Numerical simulation can also provide insight in the flow phenomena that help stabilise the detonation propagation. The previously discussed experimental results demonstrate better detonation characteristics of the RDC with the larger annular gap. In Fig. 15, an instantaneous flow structure in the cross section at 12 mm from the injector plane is visualised by the pressure gradient field in burnt gases and the temperature field in the fresh mixture ($T < 1000 \, \text{K}$). The detonation front propagates within the outer part of the cross section where the fresh mixture is located, in agreement with the chemiluminescence image in Fig. 9b. There is a leading shock induced by the detonation but situated ahead of it. This leading shock compresses some fresh mixture and interacts with the detonation front, creating a triple point and providing an additional increase in pressure and temperature. Both these factors intensify the detonation wave and make its propagation more stable. Past the detonation front, the shocks from the triple point form a shock train. One of these shocks reflects from the outer wall, resulting in a secondary pressure peak observed in Fig. 11.

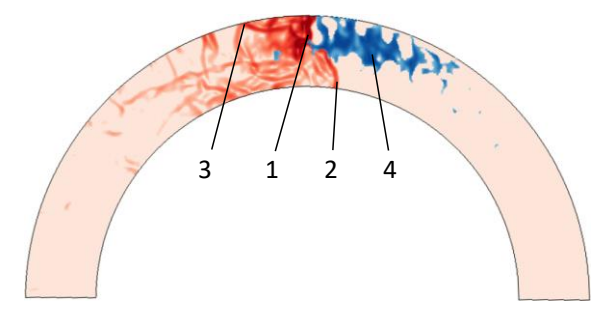


Fig 15. Flow structure in the chamber section at 12 mm from the injection plane visualized by the pressure gradient in burnt gases (red) and fresh mixture temperature (blue): 1 – detonation front, 2 – leading shock, 3 – shock reflection, 4 – fresh mixture layer

5. Conclusion

In this work, partially-premixed injection is proven to enhance mixing and detonation characteristics in a laboratory-scale RDC. The experimental results obtained with the optimized ITEM injector and the conventional TRIPLET injector were compared with published data on annular RDCs fed with CH4 and O2. This comparison showed that with the ITEM injector, it was possible to reach detonation velocity ratios up to 90% if the annular gap was large enough. Back-end chemiluminescence imaging indicated less stable propagation at a lower velocity in the 5 mm annulus.

A fairly good agreement was obtained between the experimental and simulation results regarding the pressure signals, the detonation propagation velocity, and the visualised wave structure. The simulation results confirm good mixing in front of the wave, low deflagration losses, and complete combustion at the RDC outlet. The simulation gives a detailed insight in the flow structure and help to identify the factors, stabilising the detonation wave in the wider annulus.

Acknowledgment

This study was supported by General Scientific Direction of ONERA and Region Nouvelle Aquitaine. The experiments were performed at the GAP facility of Pprime Institute, funded by the EQUIPEX program ANR-11-EQPX-0018 of the French Government. The simulation of the methane-oxygen RDC was performed using HPC resources from GENCI-IDRIS (Grant 2023-A0142B14179).

References

- 1. Wolański, P.: Detonative propulsion. Proc. Combust. Inst. 34(1), 125-158 (2013)
- 2. Davidenko, D., Eude, Y., Gökalp, I., Falempin, F.: Theoretical and numerical studies on continuous detonation wave engines. AIAA-2011-2334, 17th AIAA International Space Planes and Hypersonic Systems and Technologies Conference, San Francisco, CA (2011)
- 3. Hellard, P.: Étude numérique et expérimentale d'une chambre de combustion à détonation rotative à injection partiellement prémélangée. PhD thesis, ISAE-ENSMA (2024)
- 4. Bykovskii, F. A., Zhdan, S. A., Vedernikov, E. F.: Continuous spin detonation of hydrogen-oxygen mixtures. 1. Annular cylindrical combustors. Combustion Explosion Shock Waves 44(2), 150-162 (2008)
- Lin, W., Zhou, J., Liu, S., Lin, Z.: An experimental study on CH₄/O₂ continuously rotating 5. detonation wave in a hollow combustion chamber. Exper. Thermal Fluid Sci. 62, 122-130 (2015)
- 6. Hansmetzger, S., Zitoun, R. & Vidal, P.: A study of continuous rotation modes of detonation in an annular chamber with constant or increasing section. Shock Waves 28, 1065-1078 (2018)
- Anderson, W.A., Heister, S.D., Kan, B., Hartsfield, K.: Experimental study of a hypergolically 7. ignited liquid bipropellant rotating detonation rocket engine. J. Prop. Power 36(6), 851-861 (2020)
- 8. Goto, K., Yokoo, R., Kawasaki, A., Matsuoka K. et al.: Investigation into the effective injector area of a rotating detonation engine with impact of backflow. Shock Waves, 31(7) 753-762
- 9. Andrus, I.Q., Polanka, M.D., King, P.I., Schauer, F.R., Hoke, J.L.: Experimentation of premixed rotating detonation engine using variable slot feed plenum. J. Prop. Power 33(6), 1448-1458 (2017)
- Ayers, Z.M., Athmanathan, V., Meyer, T.R., Paxson, D.E.: Variably premixed rotating detonation 10. engine for evaluation of detonation cycle dynamics. J. Prop. Power 39(3), 351–364 (2023)
- Stechmann, D.P.: Experimental study of high-pressure rotating detonation combustion in rocket 11. environments, Ph.D. Thesis, Purdue University (2017)
- Ma, Z., Zhang, S., Luan, M., Yao, S., Xia, Z., Wang, J.: Experimental research on ignition, 12. quenching, reinitiation and the stabilization process in rotating detonation engine. Int. J. Hydroden Energy 43, 18521-18529 (2018)

- 13. Burke, R., Rezzag, T., Dunn, I., Flores, W., Ahmed, K.: The effect of premixed stratification on the wave dynamics of a rotating detonation combustor. Int. J. Hydrogen Energy 46(54), 27816-27826 (2021)
- Gaillard, T.: Étude numérique du fonctionnement d'un moteur à détonation rotative. PhD thesis, 14. Université Paris-Saclay (2017)
- Gaillard, T., Davidenko, D., Dupoirieux, F.: Numerical optimisation in non-reacting conditions of 15. the injector geometry for a continuous detonation wave rocket engine. Acta Astronautica 111, 334-344 (2015)
- Gaillard, T., Davidenko, D., Dupoirieux, F.: Numerical simulation of a rotating detonation with a 16. realistic injector designed for separate supply of gaseous hydrogen and oxygen. Acta Astronautica 141, 64-78 (2017)
- 17. Davidenko, D., Gaillard, T.: Injecteur de fluides, France Patent WO2022079368 (2020)
- Bennewitz, J.W., Bigler, B.R., Hargus, W.A., Danczyk, S.A., Smith, R.D.: Characterization of 18. detonation wave propagation in a rotating detonation rocket engine using direct highspeed imaging. Joint Propulsion Conf. (2018) https://doi.org/10.2514/6.2018-4688
- Bigler, B.R., Bennewitz, J.W., Danczyk, S.A., Hargus, W.A.: Injector mixing effects in rotating 19. detonation rocket engines. AIAA Propulsion Energy Forum (2019) https://doi.org/10.2514/ 6.2019-3869
- 20. Kindracki, J., Wolański, P., Gut, Z.: Experimental research on the rotating detonation in gaseous fuels-oxygen mixtures. Shock waves 21, 75-84 (2011)
- 21. Nair, A.P., Lee, D.D., Pineda, D.I., Kriesel, et al.: Methane-oxygen rotating detonation exhaust thermodynamics with variable mixing, equivalence ratio, and mass flux. Aerospace Sci. Technol. 113, 106683 (2021)
- 22. Bennewitz, J.W., Burr, J.R., Bigler, B.R., Burke, R.F., et al.: Experimental validation of rotating detonation for rocket propulsion. Scientific Reports 13(1), 14204 (2023)
- 23. Knowlen, C., Mundt, T., Kurosaka, M.: Experimental results for 25-mm and 51-mm rotating detonation rocket engine combustors. Shock Waves 33(3), 1–16 (2023)
- Ma, J.Z., Bao, W., Wang, J.: Experimental research of the performance and pressure gain in 24. continuous detonation engines with aerospike nozzles. Aerospace Sci. Technol. 140, 108464 (2023)
- Zhang, Y., Sheng, Z., Rong, G., Shen, D., Wu, K., Wang, J.: Experimental research on the 25. performance of hollow and annular rotating detonation engines with nozzles. Appl. Thermal Engineering 218, 119339 (2023)
- 26. Refloch, A., Courbet, B., Murrone, A., Villedieu, P., et al.: CEDRE software. Aerospace Lab J. 2, 1-10 (2011)
- 27. Laurent, C.: Low-order modeling and high-fidelity simulations for the prediction of combustion instabilities in liquid rocket engines and gas turbines. PhD thesis, INPT (2020)
- 28. Hellard, P., Gaillard, T., Davidenko, D., Zitoun, R., Vidal, P.: Numerical investigation of the effects of friction and heat transfer on a non-premixed rotating detonation combustor operation. Proc. European Combustion Meeting, 2112-2117 (2023)
- 29. Nassini, P., High-fidelity numerical investigations of a hydrogen rotating detonation combustor. PhD thesis, University of Florence (2022)